DOI:
10.1182/blood.2019001347

Document Version
Peer reviewed version

Immunobiology

Title: Treg sensitivity to FasL and relative IL-2 deprivation drive Idiopathic Aplastic Anemia immune dysfunction

Short title: Mechanism of Treg depletion in AA

Authors: Shok Ping Lim*[1], Benedetta Costantini*[1], Syed A. Mian*[1,2], Pilar Perez Abellan[1,3,] Shreyans Gandhi[3], Marc Martinez Llordella[4], Juanjo Lozano[5], Rita Antunes dos Reis[10], Giovanni A. M. Povoleri[4], Thanos P. Mourikis[6], Ander Abarrategi[2], Linda Ariza-McNaughton[2], Susanne Heck[7], Jonathan M. Irish[8], Giovanna Lombardi[9], Judith C. W. Marsh[1,3], Dominique Bonnet[2†], Shahram Kordasti[1,10,11†], Ghulam J. Mufti[1,3†]

*Joint first authors
†Joint senior authors

Affiliations:
[1]Department of Haematology, School of Cancer and Pharmaceutical Sciences, Faculty of Life Sciences and Medicine, King's College London, London, United Kingdom;
[2]Haematopoietic Stem Cell Laboratory, The Francis Crick Institute, London, United Kingdom;
[3]Haematological Medicine, King's College Hospital, London, United Kingdom;
[4]Centre for Inflammation Biology and Cancer Immunology, King's College London, London, United Kingdom;
[5]Centro de Investigación Biomédica en Red de Enfermedades Hepáticas y Digestivas (CIBERehd) Bioinformatics Platform, Madrid, Spain;
[6]Cancer Systems Biology Laboratory, The Francis Crick Institute, London, United Kingdom;
[7]National Institute for Health Research Biomedical Research Centre, BRC Flow Core, Guy's and St Thomas Hospital, London, United Kingdom;
[8]Department of Cancer Biology, Vanderbilt University, Nashville, TN;
[9]MRC Centre for Transplantation, Peter Gorer Department of Immunobiology, Faculty of Life Sciences and Medicine, King's College London, London, United Kingdom;
[10]CRUK-KHP Cancer Centre, School of Cancer and Pharmaceutical Sciences, Faculty of Life Sciences and Medicine, King's College London, London, United Kingdom
[11]Haematology Department, Guy's Hospital, London, United Kingdom

Correspondence: Shahram Kordasti and Ghulam J Mufti; Department of Haematology, School of Cancer and Pharmaceutical Sciences, Faculty of Life Sciences and Medicine, King's College London, London, United Kingdom; email: shahram.kordasti@kcl.ac.uk and ghulam.mufti@kcl.ac.uk

Text word count: 3996
Abstract word count: 234
Number of figures: 6
Number of tables: 1
Number of references: 48

Key Points

- FasL mediated apoptosis play an important role in Treg depletion and subpopulation imbalance in AA, leading to immune dysregulation.
- Remaining AA Tregs become FasL resistant in response to high concentration of IL-2 and are functional in an inflammatory environment.

Abstract

Idiopathic aplastic anemia (AA) has two key characteristics: an autoimmune response against hematopoietic stem/progenitor cells and regulatory T cells (Tregs) deficiency. We have previously demonstrated reduction in a specific subpopulation of Treg in AA, which predict response to immunosuppression. The aims of the present study were to define mechanisms of Treg subpopulation imbalance and identify potential for therapeutic intervention. We have identified two mechanisms that lead to skewed Treg composition in AA. Firstly, FasL mediated apoptosis on ligand interaction and, secondly, relative IL-2 deprivation. We have shown that IL-2 augmentation can overcome these mechanisms. Interestingly, when high concentrations of IL-2 were used for *in vitro* Treg expansion cultures, AA Tregs were able to expand. The expanded populations expressed high level of p-BCL-2, which makes them resistant to apoptosis. Using a xenograft mouse model, the function and stability of expanded AA Tregs were tested. We have shown that these Tregs were able to suppress the macroscopic clinical features and tissue manifestations of T cell-mediated graft-versus-host disease. These Tregs maintained their suppressive properties as well as their phenotype in a highly inflammatory environment. Our findings provide an insight into the mechanisms of Treg reduction in AA. We have identified novel targets with potential for therapeutic interventions. Supplementation of *ex vivo* expansion cultures of Tregs with high concentrations of IL-2 or delivery of IL-2 directly to patients could improve clinical outcomes in addition to standard immunosuppressive therapy.

Introduction

Severe aplastic anemia (AA) is a rare and potentially fatal form of bone marrow (BM) failure syndrome, characterized by peripheral blood cytopenia and hypocellular BM. Most cases of acquired AA are associated with autoimmunity.[1-3] In AA, the expansion of T effector cells ($CD4^+$ and $CD8^+$ T cells), along with the increased levels of pro-inflammatory cytokines such as interferon-gamma (IFN-γ) and tumor necrosis factor-alpha (TNF-α) results in the depletion of hematopoietic stem/progenitor cells (HSPCs).[4,5] Immune destruction of HSPCs is also associated with Fas/FasL-dependent apoptotic pathway.[6,7]

Current first-line treatment options for AA patients include hematopoietic stem cell transplantation (HSCT) for younger patients with HLA-matched sibling donors, as well as immunosuppressive therapy (IST) for older patients and patients without a matched sibling donor.[8,9] In HSCT, acute and chronic graft-versus-host diseases (GvHD) remain an issue, although occur less frequently using alemtuzumab-based conditioning.[10] Standard IST regimen using antithymocyte globulin (ATG) and cyclosporine A (CsA) has shown a response rate of 60-70% in AA patients. Nevertheless, 35% of patients relapse after responding and up to 15% of patients undergo clonal evolution to MDS and AML following IST.[3,8,9,11-13] More recently, the addition of thrombopoietin receptor agonist (Eltrombopag) to the standard IST has shown a high rate of complete response among patients with severe AA, but the relapse rate and clonal evolution were comparable to standard IST therapy.[14]

Regulatory T cells (Tregs), are an integral part of a balance immune response in human[15] and the insufficient number or function of Tregs is the major finding in most autoimmune conditions.[16] Our group and others have previously demonstrated that in AA, the number of Tregs are reduced and their function is compromised.[4,17-19] We have described two subpopulations of human Tregs with distinct immunological phenotypes, known as Treg-A (naïve phenotype with low proliferation index) and B (memory phenotype with

moderate/high proliferation index) and shown that the reduced number of Treg B correlates with inferior response to IST [20].

In the present study, we investigated the mechanisms behind the Treg reduction in AA and potential interventions which could overcome this mechanism. We found that Treg-A from AA patients were resistant to FasL-induced apoptosis and do not respond to low concentration of IL-2. However, Treg-A and B isolated from AA patients were able to expand *in vitro* and these expanded Tregs were not only functional and stable, but also expressed high level of p-BCL-2 and resistant to FasL-induced apoptosis. These findings represent potential targets to overcome AA immune dysregulation in a more targeted way and improve clinical outcome in addition to standard immunosuppressive therapy.

Methods

Study approval

King's College Hospital Local Research Ethics Committee approved this study for sample collection, and informed written consent was obtained from patients.

Patient samples

A total of 19 AA patients were involved in this study (Table 1). Peripheral blood mononuclear cells (PBMCs) from 19 AA patient samples collected at diagnosis and post IST (5 patients) and 25 healthy donors were used for various *in vitro* functional assays and *in vivo* experiments.

In vitro Treg expansion

Treg expansion *in vitro* was performed as previously described.[20,21] Total Tregs, Treg-A and Treg-B were cultured in Prime XV T cell expansion XSFM (Irvine Scientific, Santa Ana, CA), supplemented with 5% human AB serum (Sigma Aldrich, St. Louis, MO) in the presence of 2 μM all-trans-retinoic acid (ATRA; Sigma Aldrich) and 100 nM rapamycin (LC Laboratories, Woburn, MA) for 4 to 6 weeks. Tregs were stimulated with Dynabeads human T-activator CD3/CD28 (cell:bead ratio = 1:1) (Thermo Fisher Scientific, Waltham, MA) and 1000 IU/mL of human IL-2 (Proleukin; Novartis, Basel, Switzerland). The culture was replenished every 2 days with human IL-2 and every week with culture media and Dynabeads human T-activator CD3/CD28.

Suppression assay

Suppression assay was performed as previously described.[20] T_{con} cells were stained with a fluorescent proliferation dye, CFSE (BioLegend, San Diego, CA) and co-cultured with autologous Tregs at different T_{con}:Treg ratios (8:1, 4:1, 2:1 and 1:1) for 5 days in the presence of anti-CD3/CD28 beads (T_{con}:beads ratio = 20:1). Cells were harvested after 5 days and stained with Fixable Viability Dye eFluor 780 (Thermo Fisher Scientific), anti-human CD3

VioGreen (clone BW264/56; Miltenyi Biotec, Bergish Gladbach, Germany), and anti-human CD4 PerCp Cy5.5 (clone RPA-T4; BioLegend). Stained cells were analyzed on a BD FACSCanto II (BD Biosciences, San Jose, CA). FlowJo Version 7.6.5 software (Tree Star, Ashland, OR) was used to perform data analysis.

FasL-induced apoptosis assay

Treg-A and B were stimulated with 5 μg/mL of anti-Fas (clone CH11; Millipore, Burlington, MA) for 5 hours, and stained with Fixable Viability Dye eFluor 780 (Thermo Fisher Scientific) followed by Annexin V APC (BioLegend) in binding buffer (BioLegend). Stained cells were analyzed on a BD LSR Fortessa (BD Biosciences). Percentages of early (Viability Dye eFluor 780- AnnexinV+) and late (Viability Dye eFluor 780+ AnnexinV+) apoptotic cells were calculated. For rescue experiment, Treg-A and B were treated with 5 μg/mL of anti-Fas (clone CH11; Millipore) and 20 IU/mL human IL-2 (Proleukin; Novartis).

Treg sensitivity to IL-2

Treg-A and B were treated with 1, 40, 60 or 80 IU/mL of human IL-2 (Proleukin; Novartis) for 15 or 30 minutes. Protein expression level of pSTAT5, a marker for IL-2 response, was measured using western blot.

DNA methylation analysis by deep amplicon bisulphite sequencing

FoxP3 Treg-specific demethylation region (TSDR) methylation analysis using deep amplicon bisulphite sequencing was performed as previously described.[20,22] Details of the method and data analysis are included in Supplementary Methods.

RNA sequencing

Total RNA was extracted using RNeasy Mini Kit (Qiagen, Hilden, Germany) and sent to Genewiz for RNA sequencing. Details of the data analysis is included in Supplementary Methods.

Xenotransplantation

NOD/SCID/IL2rγ$^{-/-}$/IL-3/GM/SF (NSG-SGM3) mice were obtained from Dr Leonard Shultz (The Jackson Laboratory) and bred at the Francis Crick Institute biological resources facility. All animal experiments were performed in accordance to UK Home Office and Francis Crick guidelines. PBMCs and Tregs were either co-injected or injected alone into the recipient mice via the intravenous route. PBMCs and Tregs from healthy donors (HD) were co-injected in 1:1 ratio (10×10^6 cells). Due to limited number of cells available from AA patients, the number of PBMCs injected into recipient mice ranged from 1.75×10^6 to 4.5×10^6 and equal number of Tregs were co-injected together. Mice were euthanized either when animals lost 20% of body weight or at week 12. Following on, mouse tissues were recovered and analysed (see Supplementary Methods for more details).

Multi-parameter mass cytometry (CyTOF)

Cytometry by Time of Flight (CyTOF) was performed as previously described. [20] Details of the method and data analysis are included in Supplementary methods.

Statistical analysis

Statistical analysis was performed using Prism Version 7 software (GraphPad Software, La Jolla, CA). Statistical significance was calculated by *P* value using unpaired t-test. *P* value<0.05 was considered statistically significant.

Data sharing

RNA sequencing data are available at GEO (accession number is GSE140844).

Results

Treg-B are sensitive to FasL-induced apoptosis

Treg-B are characterized by high expression of CD95 (Fas), therefore we hypothesized that these Tregs are more sensitive to FasL and will undergo increased apoptosis following FasL exposure compared to Treg-A. To investigate this, we first performed RNA sequencing on Treg-A and B isolated from both HD and AA patients to explore whether Treg-B show activation of FasL-mediated apoptosis pathway. By comparing gene expression profiles of AA Treg-B to HD Treg-B using Ingenuity Pathway Analysis (IPA), the top significant upregulated pathway in AA Treg-B was apoptosis related pathways (-log *P* value=4.69; z-score=1.414) (Figure 1A, Figure S1, Table S1). In addition, one of the markedly upregulated pathways in AA Treg-B compared to AA Treg-A was death receptor signaling (-log *P* value=6.67; z-score=2.646) which includes apoptosis inducing genes and therefore, suggests previous exposure of AA Treg-B to pro-apoptotic ligands (Figure 1B and C, Figure S2, Table S2). Expression of homing receptors, including CCR4, CCR5, CCR6 and CXCR6 were also significantly increased in AA Treg-B as compared to AA Treg-A (Figure 1C). Notably, expression of *Fas* was significantly increased in 3 out of top 10 upregulated pathways in AA Treg-B (Figure 1B). Therefore, we next assessed whether Treg-B cells are more susceptible to FasL mediated apoptosis *in vitro*. We found that both early and late apoptotic rates were markedly increased in Treg-A (*P* value=0.0042) and B (*P* value=0.0001) (Figure 1D, Figure S3). However, there was a significantly higher percentage of apoptotic cells in Treg-B compared to Treg-A (*P* value=0.0041), therefore confirming that Treg-B are more sensitive to FasL-induced apoptosis than Treg-A. Interestingly, Treg-B from AA patients remain sensitive to FasL even after response to IST (Figure S4).

IL-2 responsiveness and in vitro expandability of Treg-A and B

While FasL sensitivity explains Treg-B reduction in AA, it is not clear why Treg-A, which are more resistant to FasL, cannot expand. To address this, we tested the "IL-2 responsiveness" of Treg-A *in vitro*. When Treg-A and B were treated with low concentration of IL-2 (1 IU/mL) for 15 and 30 minutes, lower pSTAT5 protein expression was observed in Treg-A compared to Treg-B (Figure 2A). However, when IL-2 concentration was increased to 40, 60 and 80 IU/mL, protein expression of pSTAT5 in Treg-A increased and was comparable to Treg-B after 30 minutes of IL-2 exposure (Figure 2B). These data suggest that Treg-A do not respond to low concentration of IL-2 but respond to higher concentration of IL-2.

When we tested the *in vitro* expandability of Tregs in a Treg-promoting culture condition[21] with high concentration of IL-2, both Treg-A and B isolated from HD and AA patients were able to expand up to 4 weeks. Expansion rates of Treg-A and B from HD were comparable (*P* value=0.6429) where Treg-A was expanded with an average of 45-fold increase (range,10.47-113.27) while Treg-B increased by 33-fold (range, 4.56-129.03) (Figure 2C). Surprisingly, for AA patients, Treg-A expanded at a significantly higher rate compared to Treg-B (*P* value=0.0198), with an average increase of 4708-fold (range, 3388.7-6027.4) compared to 185-fold increase (range, 32.39-374) (Figure 2C). Interestingly, gene set enrichment analysis (GSEA) showed that expanded AA Treg-A were significantly enriched (FDR q-value=0.0377) for cell proliferation related genes as compared to pre-expansion Treg-A (Figure 2D), which was not the case for HD Treg-A.

The next question was to understand how the *in vitro* expansion changes the Treg subpopulations. We performed Principal Component Analysis (PCA) on RNA sequencing data to study differences of transcriptional profiles of Tregs before and after *in vitro* expansion. PCA analysis showed that prior to expansion, Treg-A and B isolated from AA patients had distinct gene expression signatures with 127 significantly differential expressed

genes (FDR q-value<0.05) between them (Figure 2E, Table S3). Nevertheless, following *in vitro* expansion, although there were genes differentially expressed between the two groups, the differences were not statistically significant (Figure 2E, Table S4), suggesting that expanded Treg-A and B showed similar transcriptional profile. Using mass cytometry, we next investigated the expression of commonly expressed markers following *in vitro* expansion. Both Treg-A and B had similar expression of immune signatures where there were no significant differential markers observed between the two (Figure 2F). Interestingly, both expanded Treg-A and B were characterized by low expression of CD45RA, but high expression of CD45RO, CD95 and CCR4 (Figure 2G, Figure S5 and S6A), therefore demonstrating that they take on the immune phenotype of Treg-B.[20] Similarly, expanded total Tregs isolated from HD and AA patients showed Treg-B phenotype (Figure S6).

Stability, phenotypic plasticity and functionality of in vitro expanded Treg-A and B

To investigate the stability of *in vitro* expanded Tregs, we examined the methylation status of 15 cytosine guanine dinucleotide sites within the FoxP3 TSDR.[22] TSDR cytosine guanine dinucleotide sites in the expanded Treg-A and B from both HD as well as AA patients were highly unmethylated compared to the non-Treg ($CD4^{+}CD25^{lo}CD127^{hi}$) population (Figure 3A and B). Average methylation percentages were 7.9% for HD expanded Treg-A, 3.6% for HD expanded Treg-B, 7.4% for AA expanded Treg-A, and 12.6% for AA expanded Treg-B, compared to 89.1% for non-Treg population (Figure 3B), suggesting that expanded Tregs have stable FoxP3 expression.

Treg possess some degree of plasticity in which they are able to adapt their phenotypes and functions to changes in the environment and extracellular signals.[23-27] Hence, we studied the plasticity of expanded Tregs by culturing them in the presence of IL-1β and IL-6 that promote the secretion of IL-17A.[28,29] There were no or negligible increase in IL-17A expression in the expanded Treg-A (*P* value=0.6624) and B (P value=0.5528) as compared to

positive control ($CD4^+CD25^+$ cells) where a significant increase in IL-17A level (*P* value=0.0346) was observed (Figure 3C and D), suggesting that expanded Tregs have a stable phenotype.

To assess the functionality of expanded Tregs, fluorescent proliferation dye (CFSE)-stained conventional T cells (T_{con}) were co-cultured with autologous expanded Tregs. Both HD and AA expanded total Tregs were able to suppress the proliferation of T_{con} cells significantly at T_{con}:Treg ratios of 8:1, 4:1, 2:1 and 1:1, with no significant different in the suppressive activity between HD and AA (Figure 3E). Similarly, both expanded Treg-A and B from AA patients were able to suppress the proliferation of T_{con} cells significantly and the suppressive activity were comparable between Treg-A and B (Figure 3F and G).

High dose IL-2 induces survival of Treg-A and B by upregulating phosphorylated BCL-2

To study the mechanisms that lead to the survival of Tregs following *in vitro* expansion, we performed RNA sequencing to compare Tregs before and after expansion. IPA analysis showed that IL-2 signalling was significantly upregulated in expanded AA Treg-B in comparison to pre-expansion AA Treg-B (Figure S7). Thus, we next investigated whether IL-2 was able to rescue FasL-induced apoptosis by adding IL-2 to FasL-treated Tregs. In Treg-B, FasL-induced early and late apoptosis were rescued (*P* value=0.0022) while the FasL-mediated apoptosis of Treg-A remained low in the presence or absence of IL-2 (Figure 4A, Figure S8A). Interestingly, GSEA analysis showed that expanded Treg-A were significantly enriched (FDR q-value=0.0317) for genes associated with negative regulation of extrinsic apoptotic signalling pathway compared to Treg-A before expansion (Figure 4B). Intriguingly, *Bcl2* was significantly upregulated in 6 out of 10 enriched biological processes in expanded AA Treg-A compared to pre-expansion Treg-A (Figure S8B). Furthermore, multiplex protein assay quantifying the expression levels of various apoptotic-related proteins showed that the expression of two pro-survival proteins, p-BCL-2 and p-AKT were increased in expanded

Treg-A and B as compared to pre-expansion total Treg (Figure S8C and D). Similarly, western blot results showed that the protein level of p-BCL-2 was significantly increased (*P* value<0.05) in expanded Treg-A and B as compared to total Treg before expansion, with higher p-BCL-2 expression in AA expanded Tregs when compared to HD (Figure 4C and D). Taken together, our data suggest that when Treg-A and B are exposed to high concentration of IL-2 in *in vitro* expansion culture, elevated p-BCL-2 protein expression promotes their survival and therefore prevents FasL-derived cell apoptosis.

In vitro expanded Tregs are able to prevent GvHD in a xenograft mouse model

In order to evaluate the suppressive ability of the expanded Tregs in *in vivo*, we used our NOD/SCID/IL2rγ$^{-/-}$/IL-3/GM/SF (NSG-SGM3) humanized mice (Figure 5A). NSG-SGM3 mouse model has been previously shown to efficiently support the development and maintenance of human Tregs.[30] Firstly, to study the kinetics of human Tregs in *in vivo*, HD Tregs were transduced with a bi-cistronic vector co-expressing GFP and luciferase, and then co-injected with or without human HD CD3$^+$ cells in NSG-SGM3 mice (Figure S9A, B and C). Using whole body bioluminescence imaging, we detected Tregs for up to 5 weeks in mice that were co-injected with CD3$^+$ T cells (Figure S9C).

Next, human HD PBMC were injected into NSG-SGM3 mice with or without expanded Tregs (1:1 ratio; 10×10^6). Following on, mice that were injected with PBMC+Tregs also received additional doses of Tregs every two weeks post-injection (Figure 5A). These 2 weekly Treg injection doses were chosen based on our earlier experiment showing exhaustion of Tregs after 5 weeks (Figure S8C) in mice. Tregs or PBMC+Tregs recipient mice showed no or little clinical disease symptoms associated with xeno-GvHD. Tregs or PBMC+Tregs recipient mice had less body weight lost as compared to mice injected with PBMC alone (Figure 5B). Notably, mice injected with either Tregs or PBMC+Tregs had a significantly better overall survival compared to mice injected with PBMCs alone (Figure

5C). Following xenotransplantation, male recipient mice had a better survival than female counterparts (data not shown). Histological assessment of mouse femurs and spleen at the time of death illustrated that tissue from PBMC recipient mice had acellular bone marrow and severe disruption of tissue architecture in the BM as well as spleen (Figure 5D, Figure S10A, Figure S11). Morphological assessment of BM sections demonstrates atypical hematopoiesis with prominent fibrotic tissue in mice injected with PBMC alone. However, mice injected with Tregs with or without PBMC had normocellular marrow with no or little evidence of marrow fibrosis and Tregs were present in BM (Figure 5D, Figure S12). We next tested expanded Tregs from AA patients in NSG-SGM3 mice. Similar to HD Tregs, AA expanded Tregs (1:1 ratio; up to 4.5×10^6 cells) provided the protective effect from xeno-GvHD symptoms, and mice with either Tregs or PBMC+Tregs survived significantly longer compared to mice injected with PBMC alone (Figure 5E, Figure S10B). It is noteworthy that the GvHD suppressive ability of HD Tregs was better compared to AA Tregs., even though recipient mice with HD cells received higher doses of PBMCs (AA:1.75 - 4.5×10^6 vs HD:10×10^6).

Immune signatures and TCR clonality of the expanded Tregs pre- and post-transplanted into NSG-SGM3 mice

To study the possible changes in Tregs' immune signatures before and after xenotransplantation, we performed multi-parameter mass cytometry on expanded Tregs pre-injection and Tregs isolated from PBMC+Tregs recipient mice BM. *In vitro* expanded Tregs isolated from HD and AA patients had similar immune profiles prior to injection into mice (Figure 6A). Although we observed a significant upregulation of PD-1, Helios, Tbet and downregulation of CD62L, CD38, GATA3, CCR4, CXCR4, CD177 after xenotransplantation of HD expanded Tregs (Figure S13A), Pearson correlation analysis on median expression of 29 parameters showed that the immunological phenotypes of HD

expanded Tregs before and after xenotransplantation were similar (range of r=0.45-0.64) (Figure 6B). Similarly, there was significant downregulation of CXCR4, CCR4, CD45RO, GATA3, FoxP3, CD38, CD7 and CD161 after xenotransplantation of AA expanded Tregs (Figure S13B), however Pearson correlation analysis on median expression of 29 parameters showed similar immunological phenotypes of AA expanded Tregs before and after xenotransplantation (range of r=0.04-0.47) (Figure 6C). Interestingly, when we compared Treg B-specific markers between pre- and post-transplanted expanded Tregs, CCR4 expression was markedly reduced after xenotransplantation of both HD (P value=0.00017) and AA (P value<0.0001) expanded Tregs (Figure 6D and E, Figure S14 and S15). In addition to CCR4 expression, CD45RO (P value<0.0001) expression was also significantly downregulated after AA expanded Tregs were injected into mice (Figure 6E, Figure S15). Overall, despite some phenotypic changes following xenotransplantation, expanded Tregs from HD and AA were able to protect mice against GvHD.

To investigate the TCR clonality of the expanded Tregs before and after xenotransplantation, we performed TCR Vβ chain CDR3 high-throughput sequencing on expanded Tregs pre-injection and Tregs isolated from PBMC+Tregs recipient mice BM. The average productive clonality of the AA expanded Treg before and after xenotransplantation were 0.093 and 0.209 respectively, indicating that TCR repertoires of Treg cells are less diverse following xenotransplantation after *in-vivo* exposure to inflammatory environment (Figure 6F and G). Similarly, for HD expanded Tregs, the average productive clonality before and after xenotransplantation were 0.071 and 0.231 respectively (Figure S16).

Discussion

The reduction in the number and function of Tregs is a well-known phenomenon in AA[4,17-19], although the exact mechanism is less clear. The expansion of activated T cells as well as an increase in pro-inflammatory cytokines such as IFN-γ and TNF-α[4,5] could play an important role in preventing immunoregulatory function of Tregs and create a vicious circle of immune-dysregulation. In addition, expansion of auto-reactive T cells in AA results in destruction of HSPC, partly through the Fas/FasL cytotoxic pathway where Fas expression is enhanced on $CD34^+$ cells and FasL is upregulated in the T lymphocytes.[7,31-35] Specific subpopulation of suppressive and proliferative Tregs (Treg-B), expresses higher level of CD95 (Fas) than other less proliferative subpopulation, known as Treg-A.[20] In this study, we have demonstrated that FasL induces higher degree of apoptosis in Treg-B and these Tregs remain FasL sensitive even after response to IST. Considering the suggested role of FasL-induced progenitor cells' apoptosis in AA, it could similarly be the reason for the skewed composition of Tregs in AA patients. Although Treg-A is less sensitive to FasL, Treg-A do not expand in AA patients in the presence of low concentration of IL-2. IL-2 is a key cytokine for the Treg differentiation, functional competence and stability,[36-38] thus we hypothesized that Treg-A do not respond to physiological level of IL-2 and cannot expand in AA to compensate for overall reduction in Tregs due to FasL-induced apoptosis. Here we show that indeed Treg-A do not respond to low concentration of IL-2 and thus do not compensate for the decrease in Treg-B observed in AA.

We were able to expand Treg-A and B using high concentration of IL-2 and anti-CD3/CD28 activation beads with rapamycin and all-trans-retinoic acid (ATRA) *in vitro*. Surprisingly, we observed a markedly higher *in-vitro* expansion of Treg-A isolated from AA patients compared to Treg-B, which could be due to the removal of inhibitory effects of *in-vivo* inflammatory environment in AA that prevents Tregs function and expansion.

Following *in vitro* expansion, expanded Tregs show similarities with Treg-B both phenotypically and at gene expression level. One of the main characteristics of Treg-B is high expression of Fas and their sensitivity to FasL-mediated apoptosis. Therefore, it raises the question whether the expanded Tregs, which also express high level of Fas, remain FasL sensitive and go through apoptosis if exposed to FasL. Nevertheless, we showed that IL-2 was able to rescue FasL-induced apoptosis in expanded Tregs, indicating less sensitivity to FasL. Following expansion, Tregs express high level of pro-survival protein p-BCL-2, suggesting that expanded Tregs are able to survive in an inflammatory environment. Furthermore, there was a higher p-BCL-2 protein expression in AA expanded Tregs when compared to HD expanded Tregs, in line with the finding of higher expansion and proliferation rates in AA Tregs compared to the HD.

Adoptive Treg therapy has shown promising outcomes in several clinical settings including GvHD,[39,40] solid organ transplant rejection,[41,42] type 1 diabetes,[43-45] as well as autoimmune diseases such as systemic lupus erythematosus (SLE)[46,47] and Crohn's disease.[48] Although the subtypes of AA patients involved in this study were heterogenous, we hereby demonstrated that *in vitro* expanded Tregs from AA are functional and stable with minimal plasticity, giving the potential of using these expanded Tregs as an additional strategy to restore the Treg reduction in AA patients which may improve the clinical outcome of the standard treatment using IST. Indeed, by using NSG-SGM3 mouse model we have shown the efficacy of *in vitro* expanded Tregs in protecting mice against GvHD. While AA and HD Tregs were able to similarly suppress the proliferation of T_{con} cells *in vitro*, the efficacy of AA expanded Tregs in suppressing GvHD *in vivo* was found slightly lower than the HD expanded Tregs. This differences in the *in vivo* immunosuppressive ability of AA and HD Tregs might be due to the pre-activation of T effector cells from AA patients which were co-injected with Tregs and was not the case in HD T effector cells.[4,5] In other word, AA expanded Tregs were

inhibiting less “suppressible” T effector cells compared to HD counterparts. This could be a less problematic issue in a clinical setting where AA patients would receive IST first (i.e. ATG) that will eliminate the activated T effector cells.

This study, for the first time, delineates the mechanisms behind the skewed Tregs composition in AA which could be targeted for therapy. In addition, these findings suggest a potential role for therapy with low dose and/or low affinity IL-2 in AA as well as the potential clinical use of expanded autologous Tregs to improve patient clinical outcome in addition to the standard IST.

Acknowledgments

The authors thank the Haematology Department Tissue Bank, especially Rajani Chelliah for processing patient samples. The authors also thank The Francis Crick FACS Facility, Histopathology Facility and Biological resources facility. The authors acknowledge financial support from the Department of Health via the national Institute for Health Research (NIHR) Biomedical Research Centre awarded to Guy's & St Thomas' NHS Foundation Trust in Partnership with King's College London and King's College Hospital NHS Foundation Trust. The authors are grateful to Dr Aytug Kizilors, Dr Thomas Coats, Dr. Frederic Toulza, Dr. Stephen Orr and Jamal Anwar for their help with some experiments as well as for their scientific input.

This work is supported by a research program grant from Bloodwise UK and a grant from the Aplastic Anemia and MDS International Foundation, USA (research grant awarded to S.K.). S.K. is also supported by a grant from Cancer Research UK (Award: A29283).

Authorship Contributions

S.P.L., B.C. and S.A.M designed the study, performed experiments, analysed and interpreted data, and wrote the manuscript; P.P.A., A.A. and L.A.M. contributed to the experiments; S.G. provided clinical data; M.M.L. analyzed data and contributed in writing the paper; G.A.M.P. and T.P.M. analyzed data; S.H. provided mass cytometry data quality control; J.M.I and G.L. contributed to data interpretation and writing the paper; J.C.W.M. supervised the project and contributed to writing the paper; and D.B., S.K. and G.J.M. designed the study, supervised the project, analyzed and interpreted data, and contributed to writing the paper.

Disclosure of Conflicts of Interest

J.M.I. is a cofounder and board member at Cytobank Inc. The remaining authors declare no competing financial interests.

References

1. Young NS, Calado RT, Scheinberg P. Current concepts in the pathophysiology and treatment of aplastic anemia. *Blood*. 2006;108(8):2509.

2. Guinan EC. Diagnosis and Management of Aplastic Anemia. *ASH Education Program Book*. 2011;2011(1):76-81.

3. Young NS, Bacigalupo A, Marsh JCW. Aplastic Anemia: Pathophysiology and Treatment. *Biology of Blood and Marrow Transplantation*. 2010;16(1, Supplement):S119-S125.

4. Kordasti S, Marsh J, Al-Khan S, et al. Functional characterization of CD4+ T cells in aplastic anemia. *Blood*. 2012;119(9):2033.

5. Young NS. Pathophysiologic Mechanisms in Acquired Aplastic Anemia. *ASH Education Program Book*. 2006;2006(1):72-77.

6. Chen J, Lipovsky K, Ellison FM, Calado RT, Young NS. Bystander destruction of hematopoietic progenitor and stem cells in a mouse model of infusion-induced bone marrow failure. *Blood*. 2004;104(6):1671.

7. Liu CY, Fu R, Wang HQ, et al. Fas/FasL in the immune pathogenesis of severe aplastic anemia. *Genet Mol Res*. 2014;13(2):4083-4088.

8. Bacigalupo A. How I treat acquired aplastic anemia. *Blood*. 2017;129(11):1428.

9. Scheinberg P, Young NS. How I treat acquired aplastic anemia. *Blood*. 2012;120(6):1185.

10. Marsh JC, Gupta V, Lim Z, et al. Alemtuzumab with fludarabine and cyclophosphamide reduces chronic graft-versus-host disease after allogeneic stem cell transplantation for acquired aplastic anemia. *Blood*. 2011;118(8):2351.

11. Rosenfeld S, Follmann D, Nunez O, Young NS. Antithymocyte globulin and cyclosporine for severe aplastic anemia: Association between hematologic response and long-term outcome. *JAMA*. 2003;289(9):1130-1135.

12. Marsh JC, Bacigalupo A, Schrezenmeier H, et al. Prospective study of rabbit antithymocyte globulin and cyclosporine for aplastic anemia from the EBMT Severe Aplastic Anaemia Working Party. *Blood*. 2012;119(23):5391.

13. Passweg JR, Marsh JCW. Aplastic Anemia: First-line Treatment by Immunosuppression and Sibling Marrow Transplantation. *ASH Education Program Book*. 2010;2010(1):36-42.

14. Townsley DM, Scheinberg P, Winkler T, et al. Eltrombopag Added to Standard Immunosuppression for Aplastic Anemia. *New England Journal of Medicine*. 2017;376(16):1540-1550.

15. Josefowicz SZ, Lu L-F, Rudensky AY. Regulatory T Cells: Mechanisms of Differentiation and Function. *Annual Review of Immunology*. 2012;30(1):531-564.

16. Pellerin L, Jenks JA, Bégin P, Bacchetta R, Nadeau KC. Regulatory T cells and their roles in immune dysregulation and allergy. *Immunologic Research*. 2014;58(2):358-368.

17. Solomou EE, Rezvani K, Mielke S, et al. Deficient CD4+ CD25+ FOXP3+ T regulatory cells in acquired aplastic anemia. *Blood*. 2007;110(5):1603.

18. Shi J, Ge M, Lu S, et al. Intrinsic impairment of CD4+ CD25+ regulatory T cells in acquired aplastic anemia. *Blood*. 2012;120(8):1624.

19. Yan L, Fu R, Liu H, et al. Abnormal quantity and function of regulatory T cells in peripheral blood of patients with severe aplastic anemia. *Cellular Immunology*. 2015;296(2):95-105.

20. Kordasti S, Costantini B, Seidl T, et al. Deep phenotyping of Tregs identifies an immune signature for idiopathic aplastic anemia and predicts response to treatment. *Blood*. 2016;128(9):1193.

21. Scottà C, Esposito M, Fazekasova H, et al. Differential effects of rapamycin and retinoic acid on expansion, stability and suppressive qualities of human CD4+CD25+FOXP3+ T regulatory cell subpopulations. *Haematologica*. 2013;98(8):1291.

22. Toker A, Engelbert D, Garg G, et al. Active Demethylation of the Foxp3 Locus Leads to the Generation of Stable Regulatory T Cells within the Thymus. *The Journal of Immunology*. 2013;190(7):3180.

23. Chen Z, Barbi J, Bu S, et al. The Ubiquitin Ligase Stub1 Negatively Modulates Regulatory T Cell Suppressive Activity by Promoting Degradation of the Transcription Factor Foxp3. *Immunity*. 2013;39(2):272-285.

24. Gao Y, Tang J, Chen W, et al. Inflammation negatively regulates FOXP3 and regulatory T-cell function via DBC1. *Proceedings of the National Academy of Sciences*. 2015;112(25):E3246.

25. van Loosdregt J, Fleskens V, Fu J, et al. Stabilization of the Transcription Factor Foxp3 by the Deubiquitinase USP7 Increases Treg-Cell-Suppressive Capacity. *Immunity*. 2013;39(2):259-271.

26. Bailey-Bucktrout Samantha L, Martinez-Llordella M, Zhou X, et al. Self-antigen-Driven Activation Induces Instability of Regulatory T Cells during an Inflammatory Autoimmune Response. *Immunity*. 2013;39(5):949-962.

27. Feng Y, Arvey A, Chinen T, van der Veeken J, Gasteiger G, Rudensky Alexander Y. Control of the Inheritance of Regulatory T Cell Identity by a cis Element in the Foxp3 Locus. *Cell*. 2014;158(4):749-763.

28. Kitani A, Xu L. Regulatory T cells and the induction of IL-17. *Mucosal Immunology*. 2008;1:S43.

29. Xu L, Kitani A, Fuss I, Strober W. Cutting Edge: Regulatory T Cells Induce CD4+CD25-Foxp3- T Cells or Are Self-Induced to Become Th17 Cells in the Absence of Exogenous TGF-β. *The Journal of Immunology*. 2007;178(11):6725.

30. Billerbeck E, Barry WT, Mu K, Dorner M, Rice CM, Ploss A. Development of human CD4+FoxP3+ regulatory T cells in human stem cell factor-, granulocyte-macrophage colony-stimulating factor-, and interleukin-3-expressing NOD-SCID IL2Rγ(null) humanized mice. *Blood*. 2011;117(11):3076.

31. Omokaro SO, Desierto MJ, Eckhaus MA, Ellison FM, Chen J, Young NS. Lymphocytes with Aberrant Expression of Fas or Fas Ligand Attenuate Immune Bone Marrow Failure in a Mouse Model. *The Journal of Immunology*. 2009;182(6):3414.

32. Maciejewski J, Selleri C, Anderson S, Young N. Fas antigen expression on CD34+ human marrow cells is induced by interferon gamma and tumor necrosis factor alpha and potentiates cytokine-mediated hematopoietic suppression in vitro. *Blood*. 1995;85(11):3183-3190.

33. Maciejewski JP, Selleri C, Sato T, Anderson S, Young NS. Increased expression of Fas antigen on bone marrow CD34+ cells of patients with aplastic anaemia. *British Journal of Haematology*. 1995;91(1):245-252.

34. Luther-Wyrsch A, Nissen C, Wodnar-Filipowicz A. Intracellular Fas ligand is elevated in T lymphocytes in severe aplastic anaemia. *British Journal of Haematology*. 2001;114(4):884-890.

35. Li W, Fu J, Wang F, Yu G, Wang Y, Zhang X. Distinct overexpression of Fas ligand on T lymphocytes in aplastic anemia. *Cell Mol Immunol*. 2004;1(2):142-147.

36. Malek TR. The Biology of Interleukin-2. *Annual Review of Immunology*. 2008;26(1):453-479.

37. Boyman O, Sprent J. The role of interleukin-2 during homeostasis and activation of the immune system. *Nature Reviews Immunology*. 2012;12:180.

38. Liao W, Lin J-X, Leonard Warren J. Interleukin-2 at the Crossroads of Effector Responses, Tolerance, and Immunotherapy. *Immunity*. 2013;38(1):13-25.

39. Cao T, Soto A, Zhou W, et al. Ex vivo expanded human CD4+CD25+Foxp3+ regulatory T cells prevent lethal xenogenic graft versus host disease (GVHD). *Cellular Immunology*. 2009;258(1):65-71.

40. Trenado A, Sudres M, Tang Q, et al. Ex Vivo-Expanded CD4+CD25+ Immunoregulatory T Cells Prevent Graft-versus-Host-Disease by Inhibiting Activation/Differentiation of Pathogenic T Cells. *The Journal of Immunology*. 2006;176(2):1266.

41. Sagoo P, Ali N, Garg G, Nestle FO, Lechler RI, Lombardi G. Human Regulatory T Cells with Alloantigen Specificity Are More Potent Inhibitors of Alloimmune Skin Graft Damage than Polyclonal Regulatory T Cells. *Science Translational Medicine*. 2011;3(83):83ra42.

42. Romano M, Tung SL, Smyth LA, Lombardi G. Treg therapy in transplantation: a general overview. *Transplant International*. 2016;30(8):745-753.

43. Bluestone JA, Buckner JH, Fitch M, et al. Type 1 diabetes immunotherapy using polyclonal regulatory T cells. *Science Translational Medicine*. 2015;7(315):315ra189.

44. Marek-Trzonkowska N, Myśliwiec M, Dobyszuk A, et al. Therapy of type 1 diabetes with CD4+CD25highCD127-regulatory T cells prolongs survival of pancreatic islets — Results of one year follow-up. *Clinical Immunology*. 2014;153(1):23-30.

45. Marek-Trzonkowska N, Myśliwiec M, Dobyszuk A, et al. Administration of CD4+CD25highCD127- Regulatory T Cells Preserves β-Cell Function in Type 1 Diabetes in Children. *Diabetes Care*. 2012;35(9):1817.

46. Scalapino KJ, Tang Q, Bluestone JA, Bonyhadi ML, Daikh DI. Suppression of Disease in New Zealand Black/New Zealand White Lupus-Prone Mice by Adoptive Transfer of Ex Vivo Expanded Regulatory T Cells. *The Journal of Immunology*. 2006;177(3):1451.

47. Weigert O, von Spee C, Undeutsch R, Kloke L, Humrich JY, Riemekasten G. CD4+Foxp3+ regulatory T cells prolong drug-induced disease remission in (NZBxNZW) F1 lupus mice. *Arthritis Research & Therapy*. 2013;15(1):R35.

48. Desreumaux P, Foussat A, Allez M, et al. Safety and Efficacy of Antigen-Specific Regulatory T-Cell Therapy for Patients With Refractory Crohn's Disease. *Gastroenterology*. 2012;143(5):1207-1217.e1202.

Table

Table 1: Patients' Characteristics at Diagnosis

Characteristics	Value
Number of patients	19
Sex	
Male	11
Female	8
Disease severity at diagnosis	
VSAA	5
SAA	8
NSAA	6
PNH clone	
Yes	11
No	7
Unknown	1
Size of PNH clone, % (range)	
Red cells	0.02-0.15
Granulocytes	0.003-29.3
Monocytes	0.4-25.7
Etiology	
Idiopathic	19
Treatment	
IST	12
Eltrombopag	2
IST + Eltrombopag	1
Allogeneic stem cell transplantation	1
No treatment	3
Response to IST treatment	
CR	2
PR	6
NR	4

CR, complete response; IST, immunosuppressive therapy; NR, non-response; NSAA, non-severe aplastic anaemia; PNH, paroxysmal nocturnal haemoglobinuria; PR, partial response; SAA, severe aplastic anaemia; VSAA, very severe aplastic anaemia.

Figure Legends

Figure 1: Treg-B are sensitive to FasL-induced apoptosis. (A) Ingenuity pathway analysis comparing Treg B isolated from AA patients (n=3) to Treg B isolated from HD (n=2) shows the ranking of top 10 significant upregulated canonical pathways by -log (*P* value). Red indicates positive z-score, grey indicates zero z-score and blue indicates negative z-score. (B) Ingenuity pathway analysis on the RNA sequencing data shows the ranking of top 10 canonical pathways by -log (*P* value) in AA Treg-B (n=3) compared to AA Treg-A (n=3). Significant upregulation of *Fas* in 3 out of 10 pathways is indicated. (C) Volcano plot shows the significant differential expressed genes in death receptor signalling (red) and the upregulation of homing receptors (yellow) in Treg-B isolated from AA patients (n=3) as compared to Treg-A (n=3). (D) The percentage of early (Viability Dye eFluor 780- AnnexinV+) and late (Viability Dye eFluor 780+ AnnexinV+) apoptotic cells in Treg-A and B before, and after treatment with 5μg/ml of anti-Fas. Error bars represent mean ± SD. * P ≤ .05; ** P ≤ .01.

Figure 2: IL-2 responsiveness and *in vitro* expandability of Treg-A and B. (A and B) Western blot analysis of STAT5 and pSTAT5 protein expression in Treg-A and B after treatment with 1, 40, 60 or 80 IU/ml of human IL-2 for 15 or 30 minutes. β-ACTIN protein level is used as a loading control and numbers represent the densitometric quantification of STAT5 and pSTAT5 protein expression levels normalized to β-ACTIN. (C) The expansion rate of Treg-A and B from HD (n=6) and AA patients (n=3). Treg-A and B were stimulated with anti-CD3/CD28 beads (1 cell:1 bead ratio) and 1000 IU/mL IL-2 for 4 weeks with 2μM ATRA and 100nM rapamycin in Prime XV T cell expansion XSFM medium. Error bars represent mean ± SD. * P ≤ .05; ns P= not significant. (D) GSEA enrichment plot shows the significant enrichment of gene set for cell proliferation in AA expanded Treg-A compared to Treg-A before expansion. However, gene set of cell proliferation was not enriched in

expanded HD Treg-A as compared to pre-expansion Treg-A. This finding suggests the higher "expansion potential" of AA Treg-A compared to HD Treg A. ES, enrichment score; NES, normalized enrichment score. (E) PCA analysis on transcriptional profiles in AA Treg-A as well as B before and after expansion. (F) Chart shows the median expression of 29 markers measured by CyTOF analysis in HD expanded Treg-A (n=3) and B (n=3). Error bars represent mean ± SD. (G) Heatmap shows the median expression of Treg-B-specific markers (CD45RA, CD45RO, CD95 and CCR4) in HD Treg-A (n=3) and B (n=3) before and after expansion.

Figure 3: Stability, plasticity and functionality of *in vitro* expanded Treg-A and B. (A) Representative methylation status of TSDR in HD expanded Treg-A, HD expanded Treg-B, AA expanded Treg-A and AA expanded Treg-B compared to non-Treg. (B) Bar chart shows the percentage of methylation in HD expanded Treg-A (n=2), HD expanded Treg-B (n=2), AA expanded Treg-A (n=3), AA expanded Treg-B (n=3) and non-Treg (n=2). (C) Representative plots show the percentage of IL-17A$^+$ population in expanded Treg-A and B cultured with anti-CD3/CD28 beads (Treg:bead ratio = 6.25:1), 10 ng/ml IL-1b, 25 ng/ml IL-6 and 10 IU/ml IL-2 for 5 days and stimulated with Leukocyte Activation Cocktail, with BD GolgiPlug. The X-axis indicates log fluorescence intensity of IL-17A APC. (D) Chart shows the mean fluorescence intensity (MFI) quantification of IL-17A staining. Error bars represent mean ± SD. * $P \leq .05$; ns P= not significant. (E) The percentage of proliferation of CFSE-stained T_{con} cells when co-cultured with autologous HD and AA expanded total Tregs in 8:1, 4:1, 2:1 and 1:1 T_{con}: Treg ratios for 5 days in the presence of anti-CD3/CD28 beads (Treg: beads= 20:1). (F) The proliferation index of CFSE stained T_{con} cells when co-cultured with autologous AA expanded Treg-A or B in 8:1, 4:1, 2:1 and 1:1 T_{con}: Treg ratios for 5 days in the presence of anti-CD3/CD28 beads (Treg: beads= 20:1). Error bars represent mean ± SD. ** $P \leq .01$; *** $P \leq .001$. (G) Representative proliferation plots of CFSE stained T_{con} cells

when co-cultured with autologous AA expanded Treg-A and B in different T_{con}: Treg ratios (8:1, 4:1, 2:1 and 1:1).

Figure 4: Upregulation of phosphorylated BCL-2 in *in vitro* expanded Treg-A and B. (A) The percentage of early (Viability Dye eFluor 780- AnnexinV+) and late (Viability Dye eFluor 780+ AnnexinV+) apoptotic cells in FasL-induced Treg-A and B before and after treatment with 20 IU/mL of human IL-2. Error bars represent mean ± SD. * $P \leq .05$; ns P= not significant. (B) GSEA enrichment plot shows the significant enrichment of gene set for negative regulation of extrinsic apoptotic signalling pathway in AA expanded Treg-A as compared to Treg-A before expansion. ES, enrichment score; NES, normalized enrichment score. (C) Western blots show the BCL-2 and p-BCL-2 (Ser70) protein expression levels in HD and AA expanded Treg A and B in comparison to HD total Treg pre-expansion. β-ACTIN protein level is used as a loading control. (D) Densitometric quantification of p-BCL-2 (Ser70) protein expression level normalized to β-ACTIN. Error bars represent mean ± SD. * $P \leq .05$.

Figure 5: *In vitro* expanded Tregs suppress GvHD in NSG-SGM3 mice. (A) Schematic representation of isolation of Tregs, followed by xenotransplantation and downstream analysis. (B) Measurement of body weight loss (representing GvHD disease clinical feature) in recipient mice that were injected with HD derived PBMCs without (n=14) or with Tregs (autologous or allogenic) (n=9) or Tregs alone (n=3). (C) Overall survival of mice that were injected with HD derived PBMCs without (n=14) or with Tregs (autologous or allogenic) (n=9) or Tregs alone (n=3). (D) Representative histology tissue sections of the mouse femur bone and spleen. (E) Overall survival of mice that were injected with AA patient derived PBMCs without (n=5) or with AA Tregs (autologous or allogenic) (n=8) or AA Tregs alone (n=2).

Figure 6: Immune signatures and TCR clonality of the expanded Tregs before and after xenotransplantation into NSG-SGM3 mice. (A) CyTOF analysis shows the relative median expression of the 29 markers in HD (n=3) and AA (n=4) expanded total Tregs. (B) Heatmap of similarity matrix between pre- (n=4) and post-injection (n=4) of HD expanded Tregs based on 29 parameters, computed as Pearson correlation coefficient. (C) Heatmap of similarity matrix between pre- (n=3) and post-transplantation (n=3) of AA expanded Tregs into NSG-SGM3 mice based on 29 parameters, computed as Pearson correlation coefficient. (D) Heatmap of CyTOF analysis shows the comparison of the median expression of markers that defined Treg-B (CD45RA, CD45RO, CD95 and CCR4) between pre- (n=4) and post-transplanted (n=4) HD expanded Tregs. *** $P \leq .001$. (E) Heatmap shows the comparison of the median expression of Treg-B-specific markers (CD45RA, CD45RO, CD95 and CCR4) between pre- (n=3) and post-transplanted (n=3) AA expanded Tregs. *** $P \leq .001$. (F) Productive clonality of the TCR repertoires of AA expanded Tregs before (n=3) and after (n=3) xenotransplantation into NSG-SGM3 mice. Values near 1 represent samples with one or a few predominant rearrangements (monoclonal or oligoclonal samples) dominating the observed repertoire. Clonality values near 0 represent more polyclonal samples. (G) Representative pie charts show the diversity of TCR Vβ CDR3 in AA expanded Tregs before and after xenotransplantation into NSG-SGM3 mice.

Visual Abstract

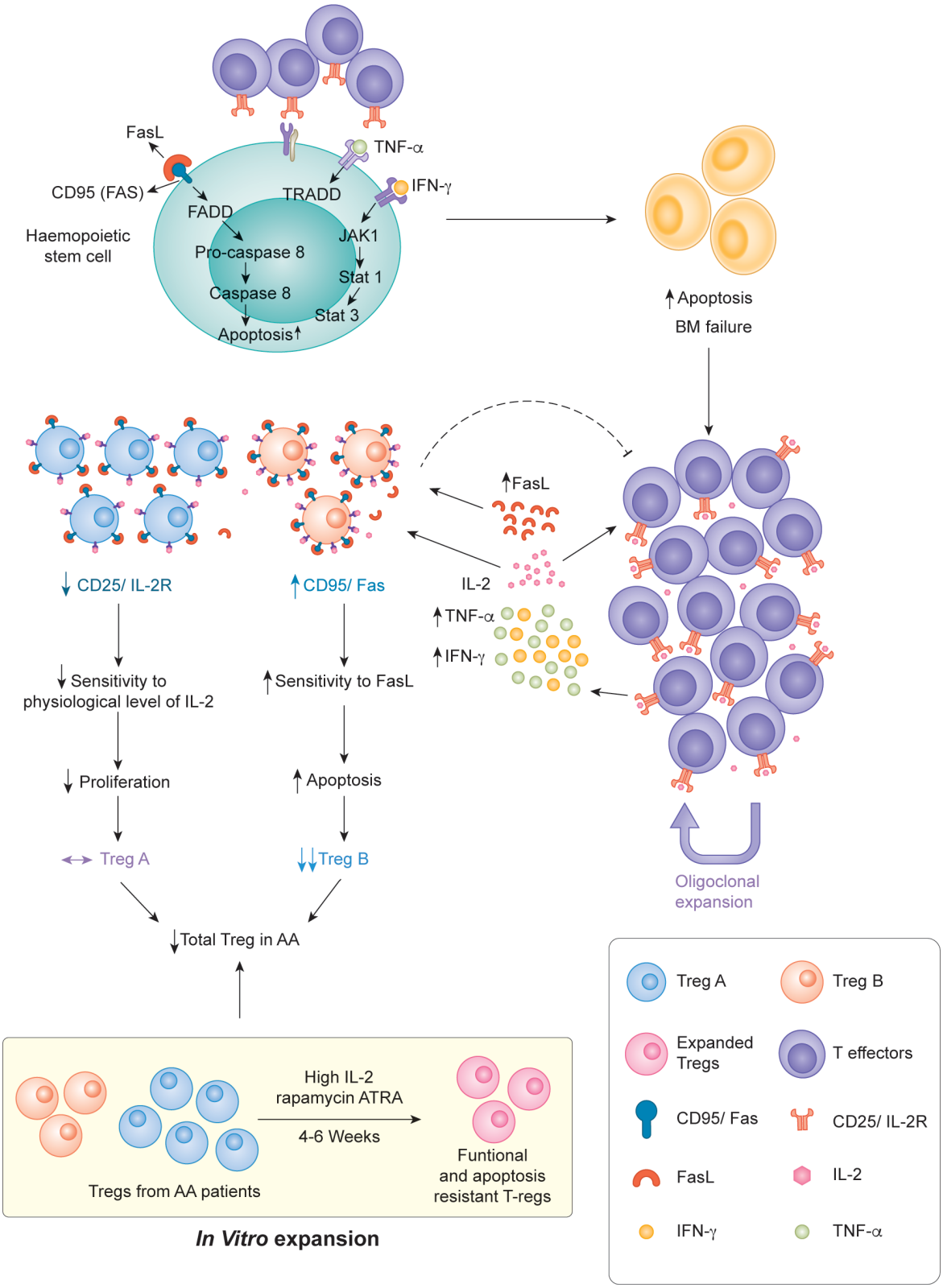
FasL
TNF-α
CD95 (FAS)
TRADD
IFN-γ
FADD
JAK1
Haemopoietic stem cell
Pro-caspase 8
Stat 1
Caspase 8
Stat 3
Apoptosis↑
↑Apoptosis
BM failure
↑FasL
IL-2
↑TNF-α
↑IFN-γ
↓CD25/ IL-2R
↑CD95/ Fas
↓Sensitivity to physiological level of IL-2
↑Sensitivity to FasL
↓Proliferation
↑Apoptosis
↔ Treg A
↓↓Treg B
Oligoclonal expansion
↓Total Treg in AA
High IL-2
rapamycin ATRA
4-6 Weeks
Tregs from AA patients
Funtional and apoptosis resistant T-regs
In Vitro expansion
Treg A
Treg B
Expanded Tregs
T effectors
CD95/ Fas
CD25/ IL-2R
FasL
IL-2
IFN-γ
TNF-α

Figure 1

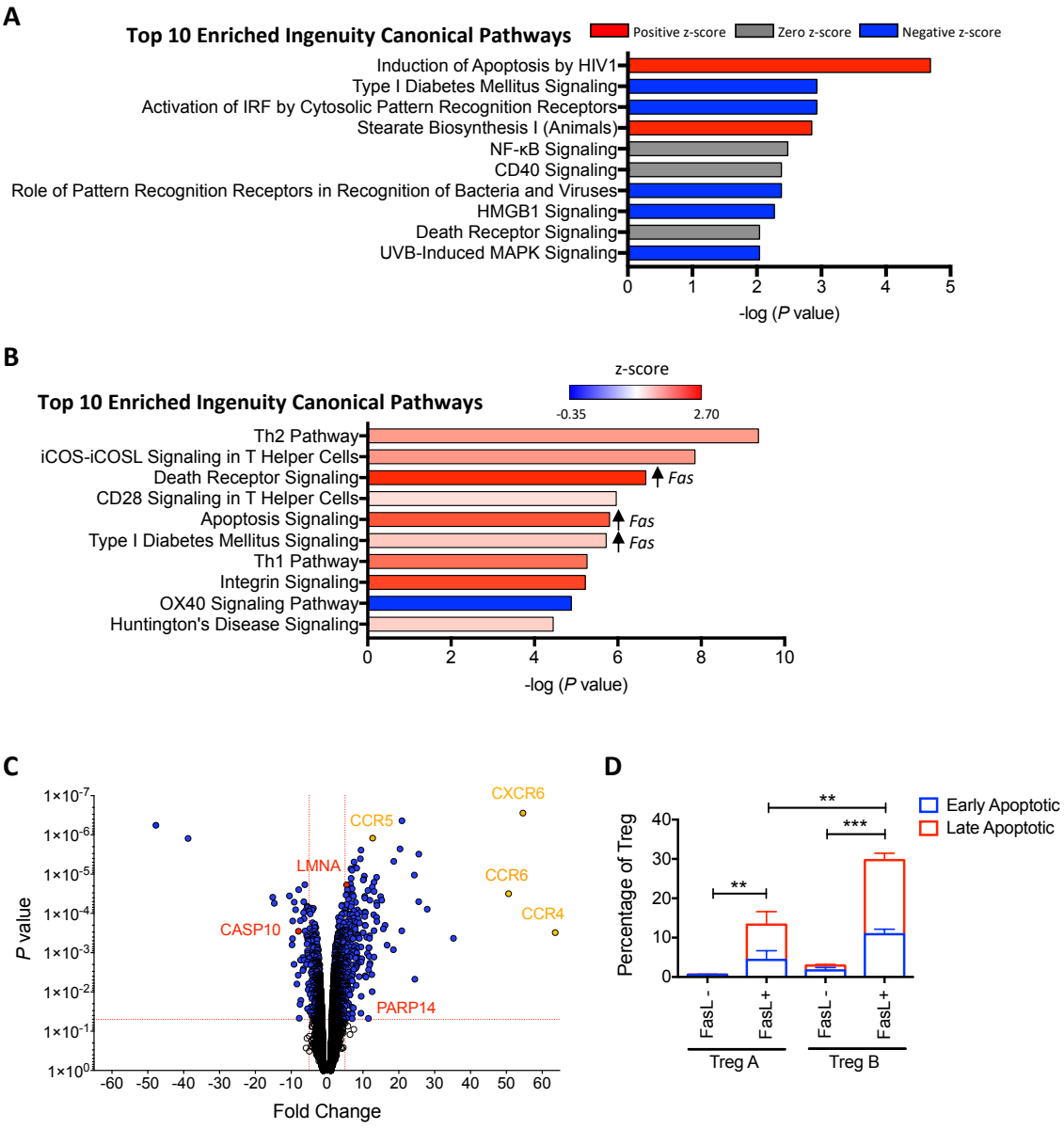
A
Top 10 Enriched Ingenuity Canonical Pathways
Positive z-score
Zero z-score
Negative z-score
Induction of Apoptosis by HIV1
Type I Diabetes Mellitus Signaling
Activation of IRF by Cytosolic Pattern Recognition Receptors
Stearate Biosynthesis I (Animals)
NF-κB Signaling
CD40 Signaling
Role of Pattern Recognition Receptors in Recognition of Bacteria and Viruses
HMGB1 Signaling
Death Receptor Signaling
UVB-Induced MAPK Signaling
0 1 2 3 4 5
-log (P value)
B
Top 10 Enriched Ingenuity Canonical Pathways
z-score
-0.35
2.70
Th2 Pathway
iCOS-iCOSL Signaling in T Helper Cells
Death Receptor Signaling
Fas
CD28 Signaling in T Helper Cells
Apoptosis Signaling
Fas
Type I Diabetes Mellitus Signaling
Fas
Th1 Pathway
Integrin Signaling
OX40 Signaling Pathway
Huntington's Disease Signaling
0 2 4 6 8 10
-log (P value)
C
P value
1×10-7
1×10-6
1×10-5
1×10-4
1×10-3
1×10-2
1×10-1
1×100
CXCR6
CCR5
LMNA
CCR6
CCR4
CASP10
PARP14
-60 -50 -40 -30 -20 -10 0 10 20 30 40 50 60
Fold Change
D
Early Apoptotic
Late Apoptotic
Percentage of Treg
0 10 20 30 40
**
***
**
FasL -
FasL +
FasL -
FasL +
Treg A
Treg B

Figure 2

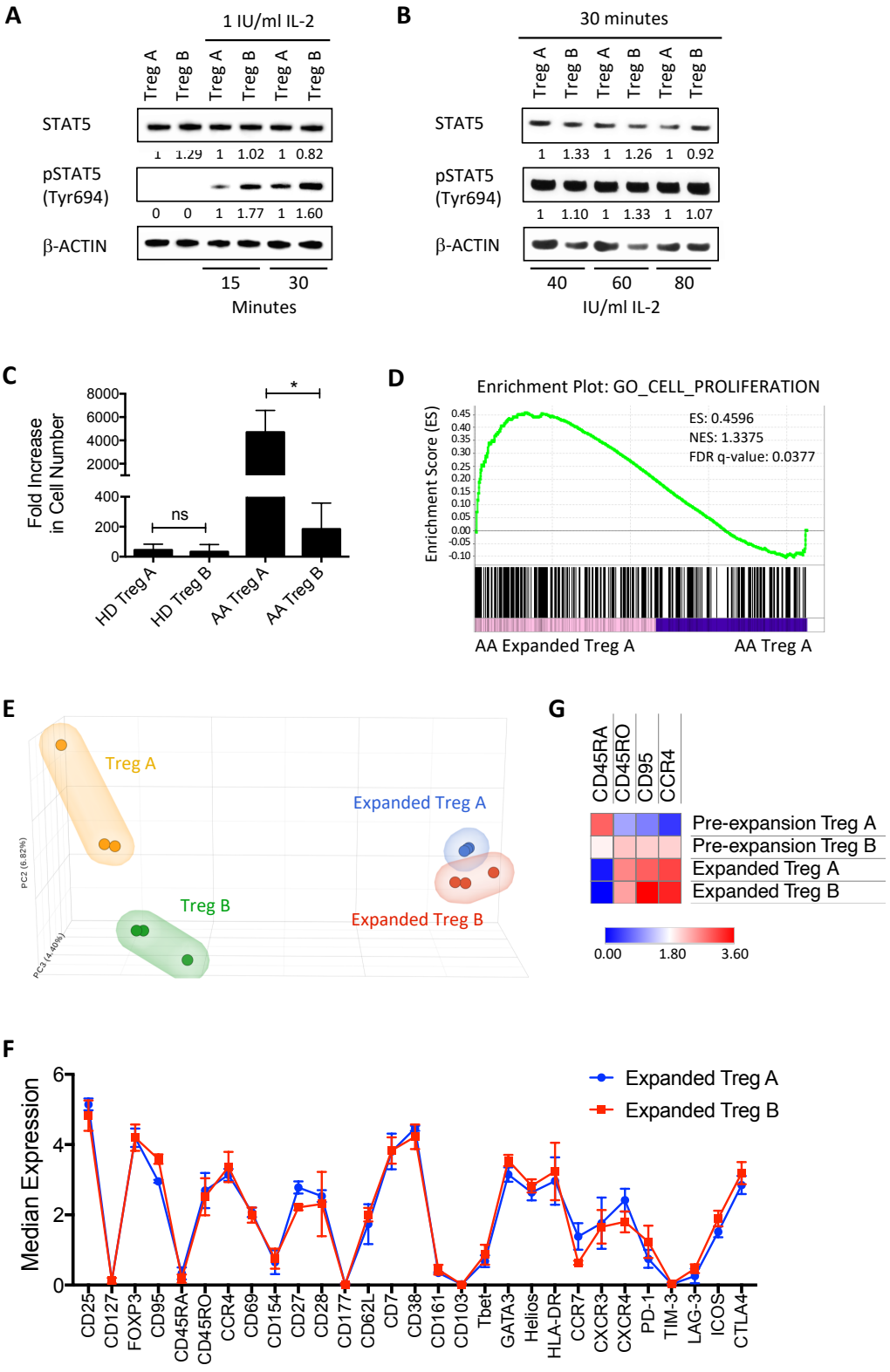
A
1 IU/ml IL-2
Treg A
Treg B
Treg A
Treg B
Treg A
Treg B
STAT5
1 1.29 1 1.02 1 0.82
pSTAT5 (Tyr694)
0 0 1 1.77 1 1.60
β-ACTIN
15
30
Minutes
B
30 minutes
Treg A
Treg B
Treg A
Treg B
Treg A
Treg B
STAT5
1 1.33 1 1.26 1 0.92
pSTAT5 (Tyr694)
1 1.10 1 1.33 1 1.07
β-ACTIN
40
60
80
IU/ml IL-2
C
Fold Increase in Cell Number
8000
6000
4000
2000
400
200
0
ns
*
HD Treg A
HD Treg B
AA Treg A
AA Treg B
D
Enrichment Plot: GO_CELL_PROLIFERATION
Enrichment Score (ES)
0.45
0.40
0.35
0.30
0.25
0.20
0.15
0.10
0.05
0.00
-0.05
-0.10
ES: 0.4596
NES: 1.3375
FDR q-value: 0.0377
AA Expanded Treg A
AA Treg A
E
Treg A
Expanded Treg A
Treg B
Expanded Treg B
PC2 (6.82%)
PC3 (4.40%)
G
CD45RA
CD45RO
CD95
CCR4
Pre-expansion Treg A
Pre-expansion Treg B
Expanded Treg A
Expanded Treg B
0.00
1.80
3.60
F
Median Expression
6
4
2
0
Expanded Treg A
Expanded Treg B
CD25
CD127
FOXP3
CD95
CD45RA
CD45RO
CCR4
CD69
CD154
CD27
CD28
CD177
CD62L
CD7
CD38
CD161
CD103
Tbet
GATA3
Helios
HLA-DR
CCR7
CXCR3
CXCR4
PD-1
TIM-3
LAG-3
ICOS
CTLA4

Figure 3

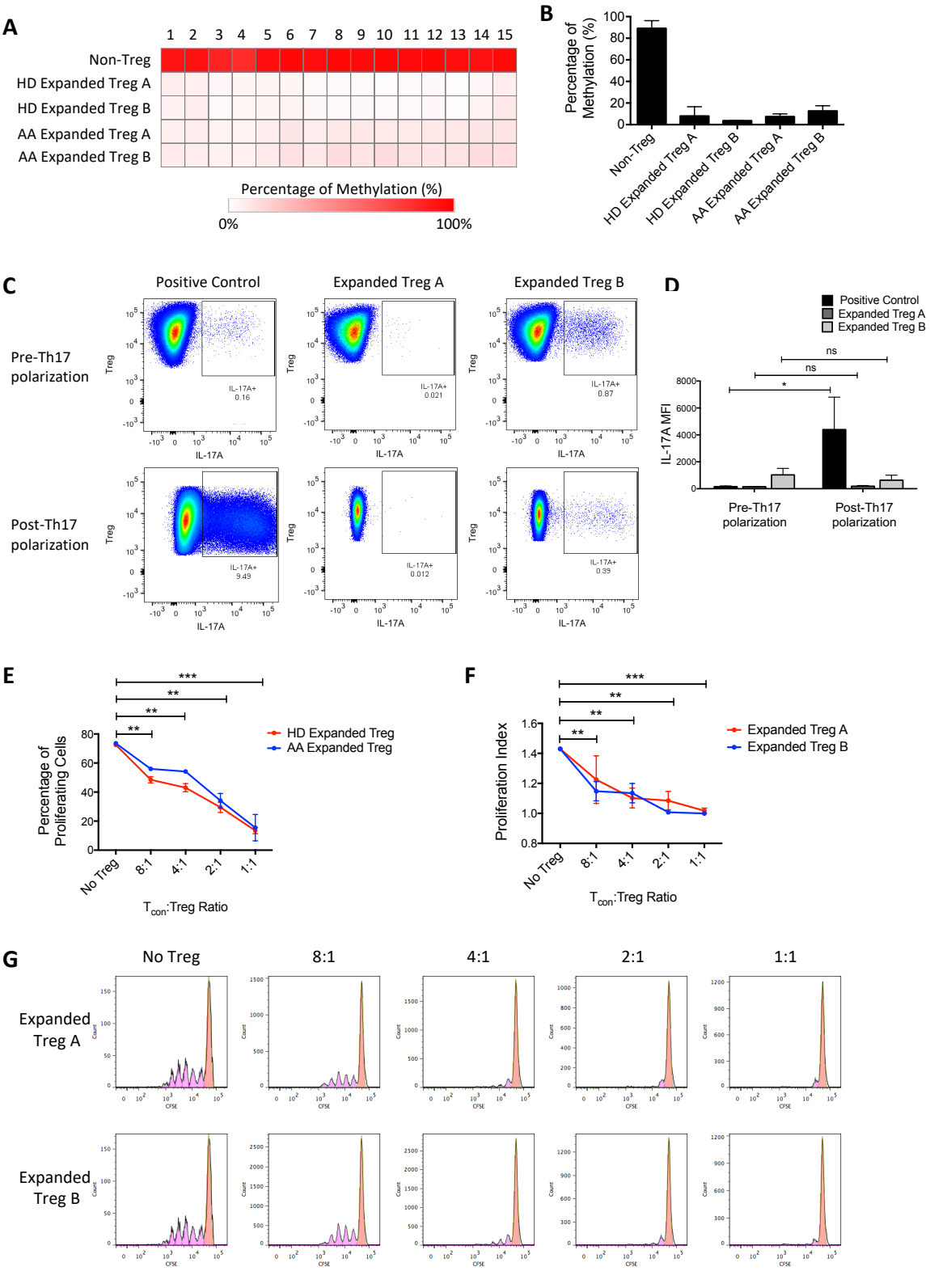
A
1 2 3 4 5 6 7 8 9 10 11 12 13 14 15
Non-Treg
HD Expanded Treg A
HD Expanded Treg B
AA Expanded Treg A
AA Expanded Treg B
Percentage of Methylation (%)
0%
100%
B
Percentage of Methylation (%)
Non-Treg
HD Expanded Treg A
HD Expanded Treg B
AA Expanded Treg A
AA Expanded Treg B
C
Positive Control
Expanded Treg A
Expanded Treg B
Pre-Th17 polarization
Post-Th17 polarization
Treg
IL-17A
IL-17A+ 0.16
IL-17A+ 0.021
IL-17A+ 0.87
IL-17A+ 9.49
IL-17A+ 0.012
IL-17A+ 0.39
D
Positive Control
Expanded Treg A
Expanded Treg B
IL-17A MFI
ns
*
Pre-Th17 polarization
Post-Th17 polarization
E
Percentage of Proliferating Cells
HD Expanded Treg
AA Expanded Treg
No Treg
8:1
4:1
2:1
1:1
Tcon:Treg Ratio
F
Proliferation Index
Expanded Treg A
Expanded Treg B
Tcon:Treg Ratio
G
No Treg
8:1
4:1
2:1
1:1
Expanded Treg A
Expanded Treg B
CFSE
Count

Figure 4

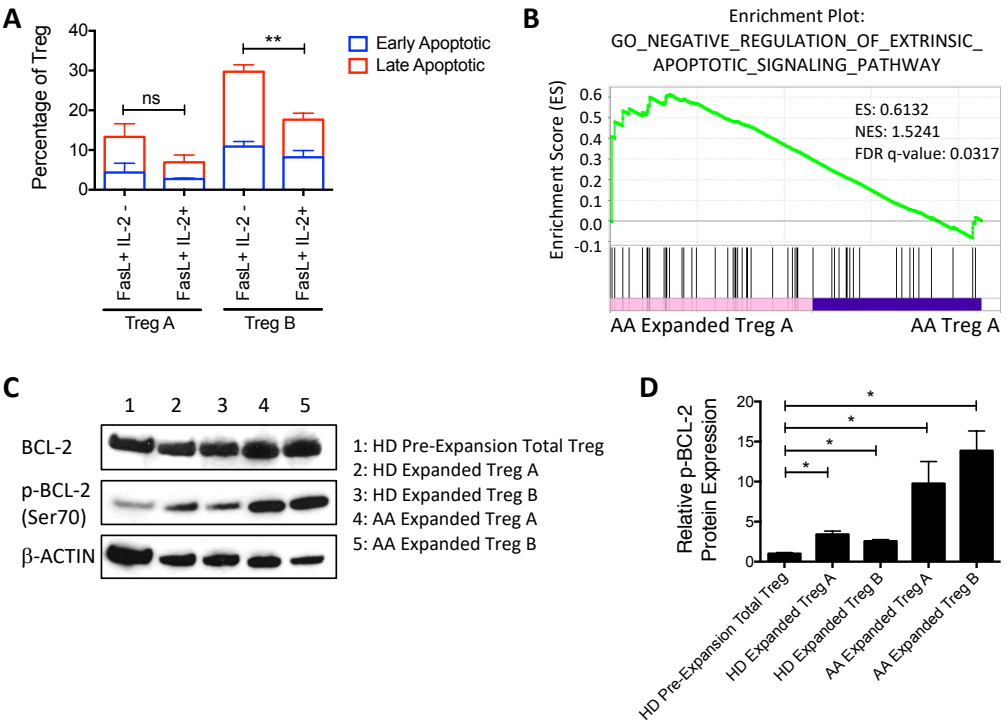
A
Percentage of Treg
40
30
20
10
0
ns
**
Early Apoptotic
Late Apoptotic
FasL+ IL-2 -
FasL+ IL-2+
FasL+ IL-2 -
FasL+ IL-2+
Treg A
Treg B
B
Enrichment Plot:
GO_NEGATIVE_REGULATION_OF_EXTRINSIC_
APOPTOTIC_SIGNALING_PATHWAY
Enrichment Score (ES)
0.6
0.5
0.4
0.3
0.2
0.1
0.0
-0.1
ES: 0.6132
NES: 1.5241
FDR q-value: 0.0317
AA Expanded Treg A
AA Treg A
C
1 2 3 4 5
BCL-2
p-BCL-2
(Ser70)
β-ACTIN
1: HD Pre-Expansion Total Treg
2: HD Expanded Treg A
3: HD Expanded Treg B
4: AA Expanded Treg A
5: AA Expanded Treg B
D
Relative p-BCL-2
Protein Expression
20
15
10
5
0
*
*
*
*
HD Pre-Expansion Total Treg
HD Expanded Treg A
HD Expanded Treg B
AA Expanded Treg A
AA Expanded Treg B

Figure 5

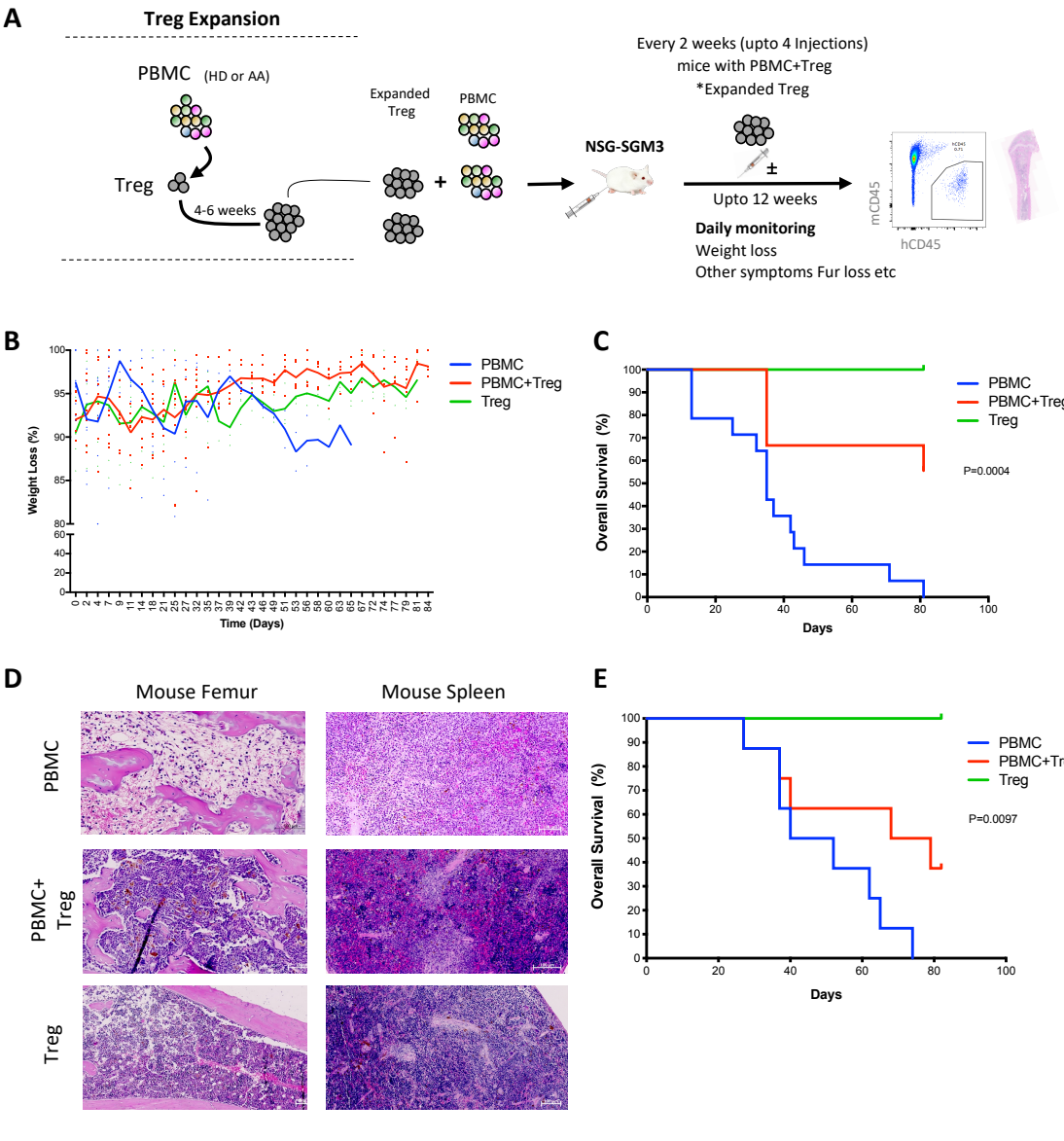
A
Treg Expansion
PBMC (HD or AA)
Treg
4-6 weeks
Expanded Treg
PBMC
NSG-SGM3
Every 2 weeks (upto 4 Injections)
mice with PBMC+Treg
*Expanded Treg
Upto 12 weeks
Daily monitoring
Weight loss
Other symptoms Fur loss etc
mCD45
hCD45
B
Weight Loss (%)
Time (Days)
PBMC
PBMC+Treg
Treg
C
Overall Survival (%)
Days
PBMC
PBMC+Treg
Treg
P=0.0004
D
Mouse Femur
Mouse Spleen
PBMC
PBMC+ Treg
Treg
E
Overall Survival (%)
Days
PBMC
PBMC+Treg
Treg
P=0.0097

Figure 6

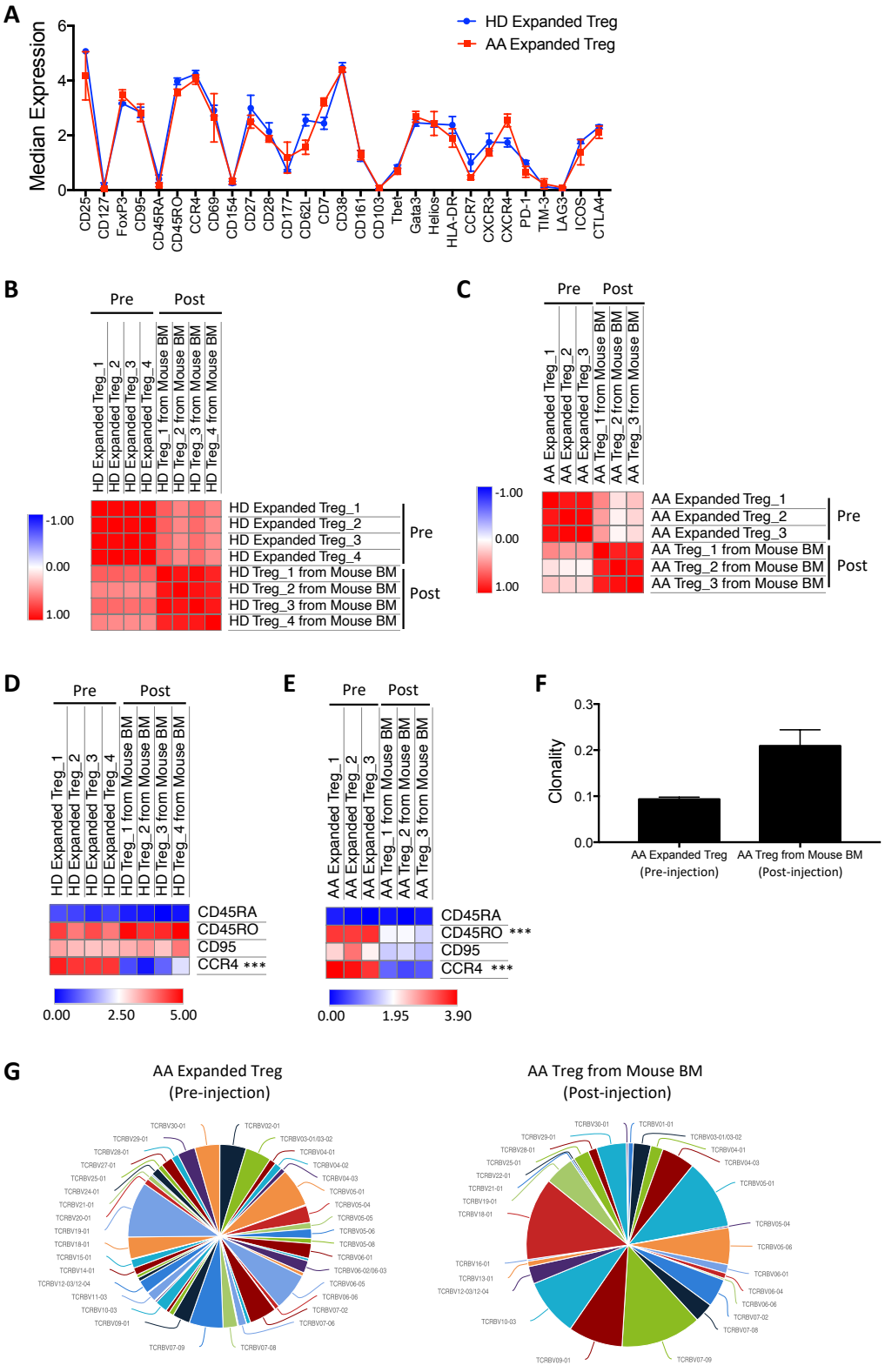
A
Median Expression
HD Expanded Treg
AA Expanded Treg
CD25
CD127
FoxP3
CD95
CD45RA
CD45RO
CCR4
CD69
CD154
CD27
CD28
CD177
CD62L
CD7
CD38
CD161
CD103
Tbet
Gata3
Helios
HLA-DR
CCR7
CXCR3
CXCR4
PD-1
TIM-3
LAG3
ICOS
CTLA4
B
Pre
Post
HD Expanded Treg_1
HD Expanded Treg_2
HD Expanded Treg_3
HD Expanded Treg_4
HD Treg_1 from Mouse BM
HD Treg_2 from Mouse BM
HD Treg_3 from Mouse BM
HD Treg_4 from Mouse BM
-1.00
0.00
1.00
C
AA Expanded Treg_1
AA Expanded Treg_2
AA Expanded Treg_3
AA Treg_1 from Mouse BM
AA Treg_2 from Mouse BM
AA Treg_3 from Mouse BM
D
CD45RA
CD45RO
CD95
CCR4 ***
0.00
2.50
5.00
E
CD45RO ***
CCR4 ***
0.00
1.95
3.90
F
Clonality
0.3
0.2
0.1
0.0
AA Expanded Treg
(Pre-injection)
AA Treg from Mouse BM
(Post-injection)
G
AA Expanded Treg
(Pre-injection)
AA Treg from Mouse BM
(Post-injection)